Positron annihilation and conductivity measurements on poly(pyrrole tosylate) and poly(pyrrole fluoride)

S. C. Sharma,* S. Krishnamoorthy, S. V. Naidu,† and C. I. Eom
Center for Positron Studies, Department of Physics, The University of Texas at Arlington, Arlington, Texas 76019

S. Krichene and J. R. Reynolds
Center for Advanced Polymer Research, Department of Chemistry, The University of Texas at Arlington, Arlington, Texas 76019

(Received 13 March 1989; revised manuscript received 25 September 1989)

Positron lifetimes, Doppler broadening of the annihilation γ energy, and electrical conductivities have been measured for two conducting polymers, poly(pyrrole tosylate) and poly(pyrrole fluoride), as functions of temperature in the range 10–295 K. The positron-lifetime spectra have been resolved into two exponentials. Positrons are localized in shallow traps, and the lifetime data suggest thermally induced detrapping of positrons at low temperatures. The temperature dependence of the conductivity has been analyzed following the variable-range-hopping model which provides results for the density of states at the Fermi energy $[N(E_f)]$ and bipolaron localization length α^{-1}. Whereas the temperature dependence of the conductivity qualitatively follows this model, it provides incorrect results for $N(E_f)$ and α^{-1}.

INTRODUCTION

Conjugated polymers have attracted substantial attention in recent years due to their remarkable electrical properties.[1–8] Unlike saturated polymers, many conjugated polymers are known to exhibit conducting behavior on oxidation-reduction (redox) doping, with conductivities as high as $10^5\Omega^{-1}\,\mathrm{cm}^{-1}$ measured for polyacetylene. A linear-chain structure makes them additionally interesting from the point of view of a reduced dimensionality, which is expected to influence their electronic properties. The electrical conductivity of these potentially technologically important materials results from mobile charge carriers introduced into their π electronic configuration. At sufficiently high-doping levels, the transport of charge is believed to occur both along the conjugated chains and via interchain hopping processes. The latter of these is used to explain the temperature dependence of the electrical conductivity in terms of the variable-range-hopping model. The intrinsic electron-phonon scattering and the many possible defects in these materials limit the transport of charge. It is, therefore, important to develop an indepth understanding of the scattering processes. Recently, there has been a growth in the scientific interest in heterocycle-based conjugated polymers based on pyrroles and thiophenes because, in addition to being reasonably good electrical conductors, they are more flexible, mechanically strong, and stable when compared with polyacetylene. They can be prepared directly in the oxidized and conducting form, using electrochemical techniques, as free-standing films removable from electrode surfaces.[9–12]

We have studied the electrical conductivity and positron annihilation parameters in poly(pyrrole tosylate) and poly(pyrrole fluoride) as functions of temperature over a wide range of temperature from 10 to 295 K. Whereas the conductivity data help us better understand the mechanism of charge transport, the positron data provide important information about the lattice distortions which facilitate conductivity in these materials. This paper presents results for the electrical conductivity and positron annihilation parameters in order to obtain complementary information about the charge transport mechanism in these materials. We discuss the electrical conductivity data in terms of the variable-range hopping of bipolarons. In the case of polypyrrole the generally accepted structure is shown in Fig. 1. The variations of the measured conductivity with temperature in both samples qualitatively follow the hopping model. However, fits of the conductivity data to the hopping model yield unacceptable results for the two important parameters of the model; the density of states at the Fermi energy $[N(E_F)]$ and the localization length α^{-1}. We compare these results with other known results and discuss possible reasons for these discrepancies. The positron-lifetime spectra have been resolved into two components with lifetimes τ_1 and τ_2. The temperature dependencies of τ_1, τ_2, and their relative intensities are discussed in terms of positron localization in shallow traps in the lattice (presumably associated with the lattice distortions responsible for conductivity, i.e., bipolarons). The positron annihilation data present the first evidence for the differences between the thermal expansion of two different microscopic regions of the same sample, existence of shallow traps, and thermally induced detrapping of positrons from these traps. The electronic structure of these two regions could be different due to the influence of the localized dopants or polymer structure and thus τ_1 and τ_2 provide important information about these regions, for example, the local electron densities. A difference in the thermal expan-

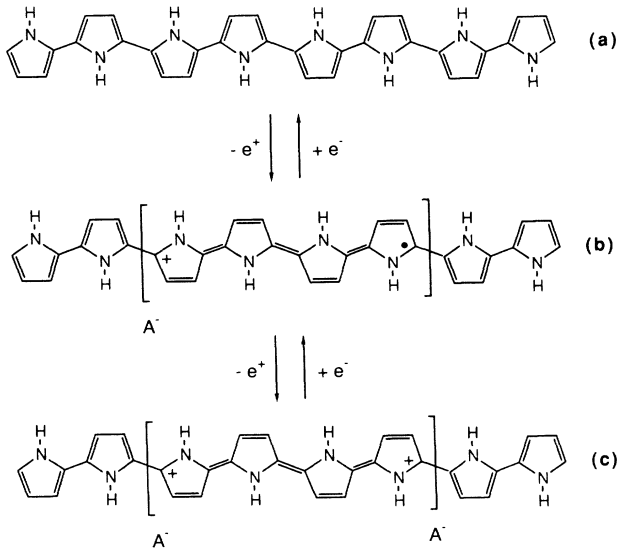

FIG. 1. (a) The structures of neutral polypyrrole, (b) polypyrrole polarons, and (c) polypyrrole bipolarons. (Dopant anion shown as A^-.)

sion of the two microscopic regions of the same sample, as evidenced by the temperature dependencies of the lifetimes, corresponds to a difference in the intermolecular interactions in these regions. This is consistent with a known concentration of the localized dopants in the sample, which should perturb the intermolecular forces in the vicinity of the dopants.

EXPERIMENT

Poly(pyrrole tosylate) films were grown by electropolymerization at a current density of 1 mA/cm^2 on a glassy carbon electrode in a one-compartment cell. The mechanism of electropolymerization of pyrrole has been studied in detail in our group.[10–13] The electrolyte consisted of acetonitrile, 2% distilled water, 0.1 M tetraethyl ammonium *p*-toluene sulfonate (TEATOS), and 0.2 M pyrrole. The electrolyte was purged with nitrogen and the polymerization was carried out under a nitrogen atmosphere for about 5 h. This resulted in a film having a thickness of about 100 μm which was thoroughly soaked and washed with acetonitrile in order to assure removal of the remaining pyrrole and excess TEATOS from the polymer film. This has been confirmed previously by elemental analysis.[9,10] Films were then dried under vacuum at 350 K for about 12 h. Poly(pyrrole fluoride) films were prepared by anion exchange of the poly(pyrrole tosylate) films as described previously using a solution of distilled water and 0.1 M NaF at room temperature.[14,15] After ion exchange the films were washed with distilled water and then dried under vacuum at 340 K for about 12 h.

The dc conductivity of the films was measured as functions of temperature by using the standard four-point technique in an Oxford Instruments helium cryostat. Positron-lifetime- spectra were measured using a fast-fast spectrometer with a full width at half maximum of $\sim$0.33 ns for the ^{60}Co prompt resolution data. Out of a total of 29 lifetime spectra, each of the 14 runs accumulated $\geq$555 000 to $\geq$762 000 counts, 10 runs accumulated $\geq$381 000 counts each, and each of the remaining 5 runs accumulated $\geq$170 000 counts. The collection time for these spectra varied due to considerations for liquid-helium consumption and due to limited access to a cryostat. These spectra were resolved into two exponential components using POSITRONFIT EXTENDED.[16] The lifetime spectra probably contain a third long-lived positronium component with a lifetime $\sim$2.2 nsec and a relative intensity $\leq$0.5%. Due to such a small intensity, this long-lived component is essentially buried in the background. These spectra also have contributions from annihilations in thin gold foils that were used to sandwich the positron source. We estimate that the source component has a lifetime $\sim$0.118 nsec with an intensity $\leq$4%. This component and its temperature dependence are, however, uncertain. We find that a correction for this short-lived source component does not significantly change the temperature dependence of the lifetime components reported in this paper. Since the source component is short lived with a rather small intensity and since the temperature effect of this component is small due to thermally generated defects in the gold foil for the temperature range of interest, we have chosen not to correct the spectra for the annihilations in the gold foils. That our data and their analyses are accurate are supported by an excellent agreement between our results and those reported by Doyle *et al.*[17] for polypyrrole samples at room temperature (details given below). The Doppler broadening of the annihilation γ-ray energy was measured by a digitally stabilized high-purity Ge detector spectrometer with an energy resolution of about 1.2 keV at 570 keV and analyzed for the standard shape parameters. The temperature of the sample was controlled with an accuracy of $\pm$1 K using the Oxford Instruments liquid-helium cryostat.

RESULTS AND DISCUSSION

The temperature dependencies of the electrical conductivity of poly(pyrrole tosylate) and poly(pyrrole fluoride) are shown in Fig. 2. Over the temperature range studied

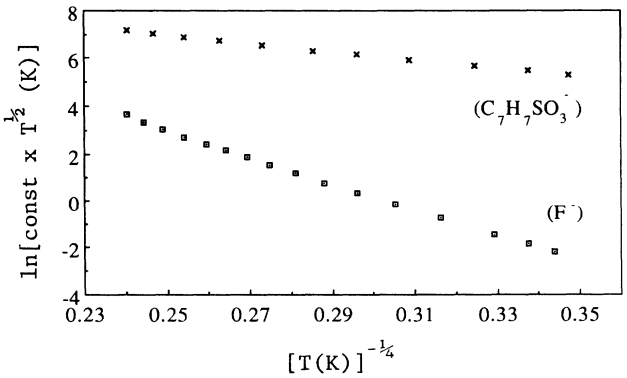

FIG. 2. Electrical conductivity as a function of temperature for poly(pyrrole) tosylate and fluoride.

from 70 to 295 K, the conductivity of each polymer increases nonlinearly with temperature. At 70 K we measure 23.9 and 0.014 $\Omega^{-1}\,cm^{-1}$ for the conductivities of the tosylate and fluoride-doped polymers, respectively. These conductivities increase to 76.3 and 2.24 $\Omega^{-1}\,cm^{-1}$ for the tosylate and fluoride samples, respectively, at 295 K. These results for the tosylate sample are in excellent agreement with the conductivities measured by others.[7,18] The ion exchange process is known to occur quantitatively.[14,15] The use of fluoride as the exchange ion causes a significant change in the electrical properties of the sample as evidenced by a lower conductivity at all temperatures. We have found that many other ions, including Cl^-, ClO_4^-, and SO_4^{2-}, have little effect on conductivity and its temperature dependence. In order to contrast the results from this study, samples with the greatest difference in properties (F^- and TOS^-) were selected for positron studies.

The temperature dependence of the conductivity in doped semiconducting samples can be explained in terms of the variable-range hopping of bipolarons.[19,20] In the simplest application of this model to conduction in amorphous solids, the phonon-assisted hopping rate of electrons is considered between two localized states, one filled at or slightly below the Fermi level, E_F, and the other empty and above the Fermi level. These two states are separated in energy by Δ and in space by R. The hopping rate is then determined by the following three factors: (i) $\exp(-\Delta/kT)$, which is proportional to the probability of finding a phonon energy Δ at a temperature T, (ii) $\exp(-2\alpha R)$, which measures the overlap for a tunneling electron between the two localized states with the same localization length α^{-1}, and (iii) an attempt frequency, ν_0, which depends on the electron-phonon coupling and the phonon density of states. The temperature dependence of the conductivity is, therefore, given by

$$\sigma=\sigma_0\exp(-A/T^{1/4}) , \tag{1}$$

where

$$\sigma_0=e^2\nu_0[N(E_F)/32\pi\alpha kT]^{1/2} , \tag{2}$$

and

$$A=2.1[\alpha^3/kN(E_F)]^{1/4} . \tag{3}$$

From Eq. (1)

$$\sigma T^{1/2}=e^2\nu_0[N(E_F)/32\pi\alpha k]^{1/2}\exp(-A/T^{1/4}) . \tag{4}$$

Following Eq. (4), we plot $\ln(\sigma T^{1/2})$ versus $T^{-1/4}$ for poly(pyrrole tosylate) and poly(pyrrole fluoride) in Fig. 2. There is a remarkable difference between the effects of temperature on the dc electrical conductivities of these two polymers. These plots agree well with Eq. (4) in that they are straight lines with a good variance of the fit. Weighted-linear-least-squares fits of these data provide the following values for α^{-1} and $N(E_F)$:

Sample	α^{-1}(Å)	$N(E_F)$ (states/eV cm^3)
Poly(pyrrole tosylate)	0.02	1×10^{27}
Poly(pyrrole fluoride)	6×10^{-8}	3×10^{29}

Though the plots of the measured conductivity shown in Fig. 2 follow an overall behavior predicted by the variable-range-hopping model via Eq. (4), the values of α^{-1} and $N(E_F)$ are, however, unreal when compared to reasonably expected values. Similar unphysical results for α^{-1} and $N(E_F)$ have also been reported by others who have studied the temperature dependence of dc electrical conductivity in similar polymers.[18,21] For example, Travers *et al.*[18] studied the temperature dependence of the conductivity in oxydized polypyrroles and substituted polypyrroles. In the substituted samples, they obtain values for α^{-1} ranging from 10^{-4} to 3×10^{-9} Å and for $N(E_F)$ ranging from 7×10^{33} to 3×10^{46} states/eV cm^3. Elliott discusses possible reasons for such anomalously high values obtained for the preexponential term in Eq. (4) that yields unphysically large values for $N(E_F)$; for example, these not-so-simple reasons may be related to the use of single-phonon theories to obtain ν_0 and to the different functional forms expected for A in Eq. (3) corresponding to hopping in three or two dimensions depending on film thickness.[19] We do not clearly understand the reasons for the anomalous results obtained by us and others for α^{-1} and $N(E_F)$. We are investigating possible effects of film thickness, dopant concentration, and morphology.

The positron lifetimes of the two components, τ_1 and τ_2, and the relative intensity of the longer-lived component, I_2, resolved in the spectra measured for

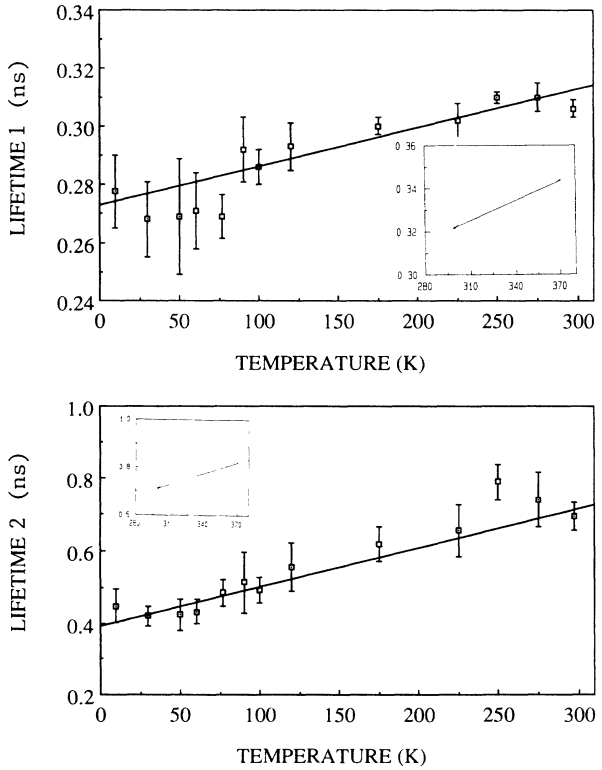

FIG. 3. Lifetime components vs temperature for poly(pyrrole) tosylate. The lines represent weighted linear least-squares fit following Eq. (10). Inset shows data from Ref. 17.

poly(pyrrole tosylate) and poly(pyrrole fluoride), are shown as functions of temperature in Figs. 3–6. For comparison, positron-lifetime results of Doyle *et al.*[17] for a polypyrrole film doped with *p*-toluenesulphonate are also represented in these figures. These authors measured positron-lifetime spectra for this sample for temperatures between 300 and 370 K. They also resolved their spectra into two lifetime components. There is excellent agreement between (i) our measurements of τ_1, τ_2, and I_2 and the results of Doyle *et al.* for these three parameters at 300 K, and (ii) extrapolated temperature dependence of our results for τ_1, τ_2, and I_2 above 300 K and the results of Doyle *et al.* Since the lifetime spectra measured in both samples can be simply resolved into two exponential components, positrons are annihilating from two different states in each sample. The lifetimes are then measures of the average electron density ($\tau \propto n_e^{-1}$) seen by positrons annihilating from each of these states. As shown by these lifetime data, the electron density in poly(pyrrole tosylate) is much lower than that in poly(pyrrole fluoride) over the entire range of temperatures. The electron density seen by positrons decreases with increasing temperature with a higher value of $|\Delta\tau/\Delta T|$ for the tosylate sample. Positrons annihilating with the longer-lifetime component probe a different microscopic region that is characterized with a much lower electron density. Whereas the electron density represented by the short-lived component is much different between the two samples over the entire temperature range, it is not the case

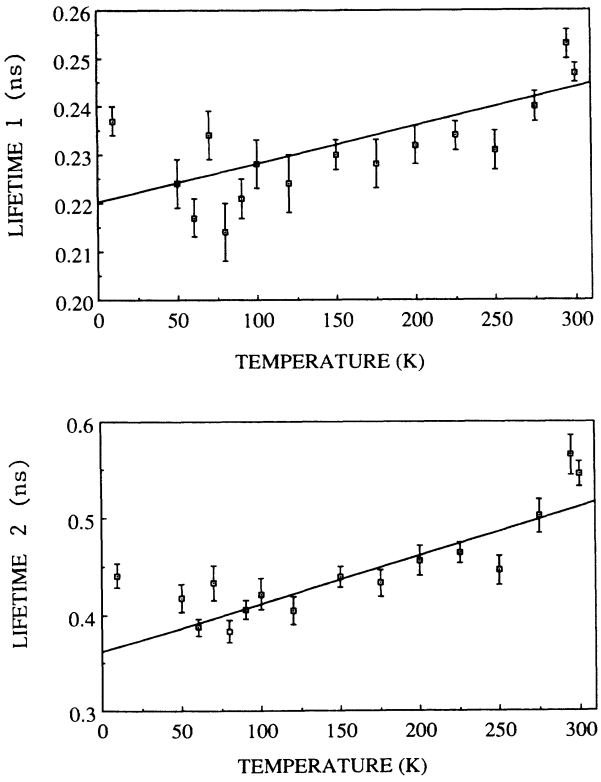

FIG. 4. Lifetime components vs temperature for poly(pyrrole) fluoride. The lines represent weighted linear least-squares fit following Eq. (10).

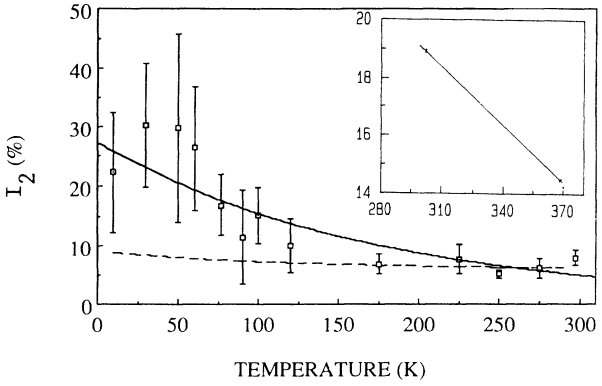

FIG. 5. The relative intensity of the longer-lived lifetime component vs temperature for poly(pyrrole) tosylate. The solid curve is drawn to aid the eye. The dashed curve represents Eq. (11) with the decay rates calculated from Eq. (10) by using the thermal expansion coefficients given in the text. Inset shows data from Ref. 17.

with the electron density of the region from which the long-lived components originate.

Following the standard two-state trapping model,[22–24] we identify τ_2 with the average lifetime of positrons trapped in lattice defects and τ_1 with the lifetime of positrons annihilating from the "free" state. At the lowest temperature (10 K) used in these experiments, the trapped positrons annihilate with a mean lifetime, $\tau_2 = 0.45 \pm 0.05$ ns with a relative intensity, $I_2 = (22 \pm 10)\%$ in the tosylate sample. The lifetime of the positrons annihilating from the free state in the tosylate sample at 10 K is $\tau_1 = 0.28 \pm 0.01$ ns. Both lifetimes τ_1 and τ_2 increase with increasing temperature; at 295 K they are measured to be 0.31 ± 0.01 ns and 0.70 ± 0.04 ns, respectively. The relative intensity of the trapped positrons increases from a value of about 22% at 10 K to about 30% at 40 K. Having reached a maximum value at 40 K, I_2 decreases with increasing temperature

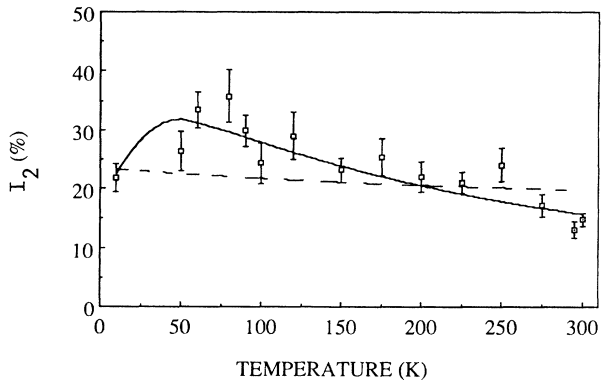

FIG. 6. The relative intensity of the longer-lived lifetime component vs temperature for poly(pyrrole) fluoride. The solid curve is drawn to aid the eye. The dashed curve represents Eq. (11) with the decay rates calculated from Eq. (10) by using the thermal expansion coefficients given in the text.

above 40 K, reaches a value of about 7.6% at 200 K, and remains at this low value between 200 and 295 K. Similar results are obtained for the poly(pyrrole fluoride) sample. In this sample, positrons annihilate from the trapped state with $\tau_2=0.44\pm0.01$ ns with a relative intensity, $I_2=(22\pm3)\%$ at 10 K. The lifetime in the free state at 10 K is $\tau_1=0.24\pm0.01$ ns. Again, the relative intensity of the trapped positrons in the fluoride sample increases from about 22% at 10 K to about 35% at 70 K. It decreases with increasing temperature above 70 K and approaches a low value of about 13% at 295 K.

The behaviors of the two lifetime components and their relative intensities with temperature observed in both polymer samples in our experiments cannot be understood in terms of a simple picture involving positron trapping only in thermally generated lattice defects. We discuss the temperature dependencies of these positron annihilation parameters based on the thermal expansion of the microscopic regions in which the positrons are localized in relatively shallow traps created by the dopants around the lowest temperature (10 K) and based on the possibility of the detrapping of positrons at higher temperatures. Unlike the case of metals in which the concentration of the positron trapping sites, i.e., point defects, is increased by raising sample temperature, the concentration of the trapping sites in our polymer samples is essentially determined by the concentration of the dopants. Since the latter was a constant for each sample , we do not expect any significant change in defect concentration over the range of temperatures between 10 and 295 K. This is consistent with relatively high values ($\sim$0.36–0.73 eV) measured for the formation energies for lattice defects in other polymers and molecular solids.[25,26] With such a high value of the formation energy, we expect a concentration of the order of only 10^{-8} for the thermally generated defects for temperatures in the range 10 to 295 K.

Also, if the above-mentioned simple trapping scenario, where positrons are trapped in thermally generated traps like in metals, were valid, then (1) the lifetime of the trapped positrons τ_2 should remain temperature independent (although a temperature effect with a negative value for $|\Delta\tau_2/\Delta T|$ has been observed in metals[27–29]). On the contrary, τ_2 is observed to increase with temperature, (2) the lifetime of the positrons annihilating from the free state τ_1 should decrease with temperature. However, we observe an increase even in τ_1 with temperature, and (3) the relative intensity of the trapped positrons I_2 should increase with temperature until saturation at some temperature corresponding to trapping of all the positrons implanted into the sample.[30] However, we observe an increase in I_2 only from 10 K to a sample-dependent temperature of $\sim$40 or 70 K. At higher temperatures I_2 decreases with increasing temperature in both samples. We have also analyzed the lifetime spectra by constraining τ_2 to a temperature-independent value. From these analyses, τ_1 turns out to be temperature independent and I_2 changes with temperature. These results are obviously in contradiction with the simple trapping model. This model provides, for reasonable values of the needed parameters (that are consistent with observed changes in I_2), a reduction of about 14% in τ_1 between 10 and 300 K.

We discuss our findings based on the following model: (i) the trapping sites for the positrons in these polymers are created as a result of spacially localized tosylate or fluoride dopant anions. These dopants create local lattice distortions in a manner so as to create "local" negatively charged regions that localize positrons, (ii) these traps are shallow and consequently the binding energy of the localized positron state is low and of the order of kT with $T=40$ and 75 K for the tosylate and fluoride samples, respectively, (iii) there is possible detrapping of positrons at temperatures higher than about 75 K, and (iv) the thermal expansion of the sample (observed to be several times larger than that of metals) further lowers electron density at the site of the positron. This results in an increase in the positron lifetimes. We, therefore, explain the positron annihilation data of Fig. 3–6 by combining simple thermal expansion of the lattice with positron trapping in shallow traps from which they can escape at sufficiently high temperatures.

Following the trapping model including a finite probability of escape of the positrons from shallow traps, the time dependence of the number of positrons is given by[31]

$$dn_f(t)/dt=-\lambda_f n_f(t)-\mu c n_f(t)+\lambda_e c n_d(t)\ , \tag{5}$$

$$dn_d(t)/dt=-\lambda_d n_d(t)+\mu c n_f(t)-\lambda_e c n_d(t)\ , \tag{6}$$

where n_f and n_d are the number of positrons in the free and trapped states; λ_f and λ_d are the decay rates from the free and the trapped states; μ is the trapping rate into the defects; λ_e is the rate of escape from the trapped state; and c is the concentration of the trapping sites. The solution of these coupled equations provides the probability $p(t)$ that the positron entering the sample at time $t=0$ has survived until time t. It is given by

$$p(t)=(\lambda_f-\Gamma_2)/(\Gamma_1-\Gamma_2)\exp(-\Gamma_1 t)+(\Gamma_1-\lambda_f)/(\Gamma_1-\Gamma_2)\exp(-\Gamma_2 t)\ , \tag{7}$$

where the rates Γ_1 and Γ_2 are given by

$$\Gamma_{1,2}=\tfrac{1}{2}(\lambda_f+\lambda_d+\mu c+\lambda_e c\pm\{[(\lambda_f+\mu c)-(\lambda_d+\lambda_e c)]^2+4\mu c^2\lambda_e\}^{1/2})\ . \tag{8}$$

The subscripts 1 and 2 on Γ refer to plus and minus signs, respectively. The relative intensity of the longer-lived component I_2 is given by

$$I_2=(\Gamma_1-\lambda_f)/(\Gamma_1-\Gamma_2)\ ,$$

$$I_2=(\lambda_d-\lambda_f+\mu c+\lambda_e c\pm\{[(\lambda_f+\mu c)-(\lambda_d+\lambda_e c)]^2+4\mu c^2\lambda_e\}^{1/2})/(2\{[(\lambda_f+\mu c)-(\lambda_d+\lambda_e)]^2+4\mu c^2\lambda_e c\}^{1/2})\ , \tag{9}$$

with

$$I_1+I_2=1 .$$

The above equations alone, however, cannot explain the observed temperature dependencies of the lifetime components shown in Figs. 3 and 4. The effect of the escape of the positrons from shallow traps should result in a shortening of the longer lifetime τ_2 and in a decrease in the value of the relative intensity of this component. The I_2 data of Figs. 5 and 6 show reductions in the relative intensities ($dI_2/dT<0$) of the longer-lifetime components measured for the two polymer samples above certain temperatures. While this is consistent with the escape picture described above, the changes seen in the lifetimes in both polymer samples with temperature are not accounted for by this picture.

We propose that the temperature dependence of the lifetime components in these polymer samples should be understood, at least to first order, in terms of the simple thermal expansion of the sample. We first evaluate the effects of the thermal expansion on the two lifetime components and the relative intensity without a consideration of the escape of the trapped positrons. The net result of this expansion is to lower the local electron density around the positron. This results in a longer lifetime as the sample temperature is increased. We, therefore, write

$$\lambda(T)=\lambda(T_0)[1+\alpha(T-T_0)]^{-3} , \tag{10}$$

where T_0 is a reference temperature and α is the coefficient for linear thermal expansion of the microscopic region seen by the positron. We make weighted least-squares fits to the temperature dependencies of τ_1 and τ_2 by using Eq. (10). This provides values for the expansion coefficients for the microscopic regions corresponding to the "free" and "trapped" states of the positron in both samples. These results are summarized below:

Sample	$\alpha_f(\mathrm{K}^{-1})$ from τ_1 free state	$\alpha_d(\mathrm{K}^{-1})$ from τ_2 trapped state
Poly(pyrrole tosylate)	$(1.6\pm0.3)\times10^{-4}$	$(9.1\pm0.1)\times10^{-4}$
Poly(pyrrole fluoride)	$(1.2\pm0.2)\times10^{-4}$	$(4.6\pm0.4)\times10^{-4}$

These results for the expansion coefficients are in very good agreement with the macroscopic coefficients for thermal expansion for similar polymer samples; for example, $\alpha=4\times10^{-4}$ and 5.5×10^{-5} for Epoxy[32] and Nylon[33] materials, respectively. This agreement, at least, suggests that a simple thermal expansion of these polymer samples is a plausible mechanism that could account for the changes seen in the positron lifetimes between 10 and 295 K. For comparison we notice that $\alpha=2.5\times10^{-5}$ and 1.66×10^{-5} for aluminum and copper, respectively. The sample region corresponding to the trapped state expands about 3.8 to 5.7 times more than the region associated with the free state of the positron. This is not surprising in view of the influence of the dopants on the local electronic structure in the localization region. Without escape, Eq. (9) provides

$$I_2=\mu c/(\lambda_f-\lambda_d+\mu c) , \tag{11}$$

where the temperature-dependent values of the decay rates are given by Eq. (10) with appropriate coefficients of thermal expansion for the two regions. Using the values of α_f and α_d given above, we calculate the relative intensity of the longer-lived component as a function of temperature. These results for I_2 are compared with the measurements in Fig. 5 and 6. The simple thermal expansion model provides, at least, decreasing values of I_2 with increasing temperature. This qualitatively agrees with the data. This simple model, however, does not agree quantitatively with the experimental results. Contrary to a linear temperature dependence predicted by the thermal expansion model, both lifetime components show a change in the value of $\Delta\tau/\Delta T$ around 70 K. In addition, a rise seen in the values of I_2 between 10 and 40 (70) K is not explained by this model.

We conjecture that a more satisfactory explanation of the temperature dependencies of the lifetime components and the relative intensity should be obtained by combining three effects: (i) thermal expansion, (ii) thermal-assisted escape of positrons from shallow traps, and (iii) possible change in the escape probability due to thermal expansion. We have already discussed and employed the thermal expansion model to fit the temperature dependencies of τ_1,τ_2, and I_2. We have also described possible effects of thermal-assisted escape of positrons on the lifetime parameters. In this regard we have also examined the temperature behavior of the positron mean lifetime, $\bar{\tau}=I_1\tau_1+I_2\tau_2$ and the bulk lifetime, $\tau_b=(I_1/\tau_1+I_2/\tau_2)^{-1}$ for the poly(pyrrole tosylate) sample. The variation of these parameters is very similar to that seen previously in the case of Cd at low temperatures.[34] Specifically, there is a change in $\Delta\tau/\Delta T$ at around 150 K and the two lifetimes ($\bar{\tau}$ and τ_b) exhibit different slopes. This agrees with the Cd results which had confirmed $dI_2/dT<0$ due to positron detrapping at low temperatures. A detailed analysis of the lifetime data following the effects listed above under (ii) and (iii), however, is not possible at this time because it requires detailed knowledge about the positron-defect interactions, temperature dependencies of the trapping and detrapping rates, and the nature of the trapping sites (vacancies, dislocations, other strain related defects, etc.).[35,36] The complexity of such an analysis is further emphasized by the known differences between the trapping and detrapping rates for the different kinds of defects (the polymer samples may contain a complex network of defects) as given below: (a) for dislocations,

$$\lambda_e/\mu=mkT/(2\rho\hbar^2)\exp(-E_b/kT)/\mathrm{erf}(\sqrt{E_b/kT})$$

(b) for surfaces,

$$\lambda_e/\mu=1/\rho(mkT/2\pi\hbar^2)^{1/2}\times\exp(-E_b/kT)/[1-\exp(-E_b/kT)] ,$$

and (c) for voids,

$$\lambda_e/\mu = 1/\rho V \exp(-E_b/kT) \times[(\sqrt{\pi}/2)\mathrm{erf}(\sqrt{E_b/kT}) - \sqrt{E_b/kT}\exp(-E_b/kT)] . \quad (12)$$

Here ρ is equal to the number of line defects per unit area for dislocations and to surface to volume ratio for surface defects, V is the volume of the trap, and E_b is the positron binding energy in the trap. The thermal effects manifest themselves in the form of lattice vibrations and lattice expansion. Both of these effects are known to influence, in a rather complicated manner, positron escape from the trapping sites. Finally, we present results on the temperature dependence of the Doppler spectra in Fig. 7. These results on the standard s parameter and the "valley-to-peak" ratio (Y parameter) are important because (1) they support our interpretation of the lifetime data and (2) they enable a test on whether the lifetime component with lifetime ≥ 500 ps is due to positronium annihilations. The temperature dependence of the s parameter clearly shows that the number of the positron trapping sites, as we have stated above, does not change according to a Boltzmann factor. The trapping sites in these samples are probably determined by the dopants. The valley-to-peak data support our view that the long-lived component is not primarily due to positronium annihilations. It is so because positronium annihilations at temperatures above a certain sample dependent temperature would manifest as an increase in the valley-to-peak ratio. The latter is not seen. On the contrary, this shows a small negative slope that remains essentially constant over the range of temperatures studied.

In summary we have presented detailed results from a series of experiments by which we have investigated the temperature dependencies of the dc electrical conductivity and positron annihilation parameters in poly(pyrrole tosylate) and poly(pyrrole fluoride) from 10 to 295 K. The major findings of these experiments are (1) the variations in the electrical conductivity with temperature qualitatively follow the variable-range-hopping model. But the same model yields unphysical results for the two important parameters α^{-1} and $N(E_F)$, (2) positrons probe two different microscopic regions in each sample and show that each region has a characteristic thermal expansion due to differences in the intermolecular interactions,

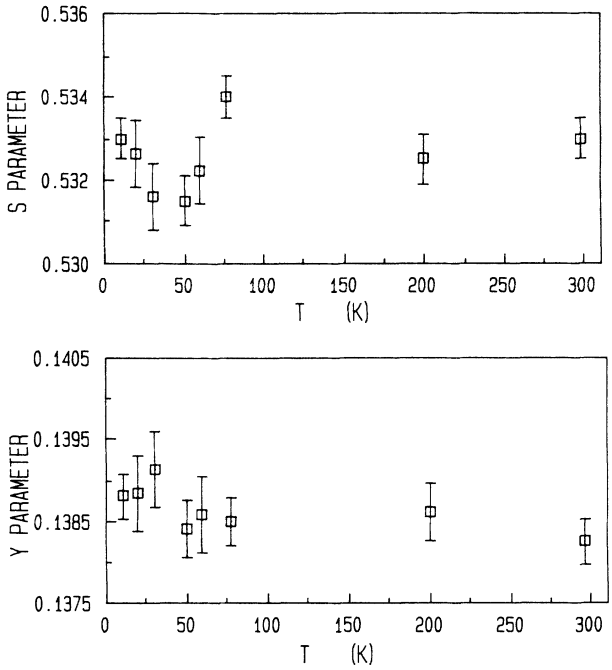

FIG. 7. The s parameter and valley-to-peak ratio for the Doppler broadening spectra vs temperature for poly(pyrrole tosylate).

(3) positrons are localized in shallow traps that are created possibly by the dopants in the polymer, and (4) the data suggest thermally induced detrapping of positrons from the traps. Whereas the conductivity data provide information about the transport of charges via lattice distortions (bipolarons), the positron data provide information about the electronic structure in the region of these distortions. It is hoped that further investigations of the results obtained from these two different experiments will complement each other so as to clarify the reasons behind the anomalous values of α^{-1} and $N(E_F)$.

ACKNOWLEDGMENTS

This research has been supported in part by grants from the Robert A. Welch Foundation, Houston, Texas (Grant No. Y-1013) and from the U.S. Defense Advanced Research Projects Agency, monitored by the Office of Naval Research, U.S. Department of Defense.

*To whom correspondence should be addressed.
†Present address: Department of Physics, Grambling State University, Grambling, LA 71245.

[1]A. J. Heeger, S. Kivelson, J. R. Schrieffer, and W.-P. Su, Rev. Mod. Phys. **60**, 781 (1988).
[2]J. R. Reynolds, J. Mol. Electron. **2**, 1 (1986).
[3]J. L. Bredas and G. B. Street, Accounts Chem. Res. **18**, 309 (1985).
[4]P. Pfluger and G. B. Street, J. Chem. Phys. **80**, 544 (1984).
[5]P. Pfluger, U. M. Gubler, and G. B. Street, Solid State Commun. **49**, 911 (1984).
[6]J. C. Scott, J. L. Brédas, K. Yakushi, P. Pfluger, and G. B. Street, Synth. Met. **9**, 165 (1984).
[7]K. K. Kanazawa, A. F. Diaz, M. T. Krounbi, and G. B. Street, Synth. Met. **4**, 119 (1982).
[8]G. B. Street, T. C. Clarke, M. Krounbi, K. Kanazawa, V. Lee, P. Pfluger, J. C. Scott, and G. Weiser, Mol. Cryst. Liq. Cryst. **83**, 253 (1982).
[9]K. J. Wynne and G. B. Street, Macromolecules **18**, 2361 (1985).
[10]J. R. Reynolds, P. A. Poropatic, and R. L. Toyooka, Macromolecules **20**, 958 (1987).
[11]S. Krishnamoorthy, M. S. thesis, The University of Texas at

Arlington, 1988 (unpublished).
[12]C. H. Huang, M. S. thesis, The University of Texas at Arlington, 1986 (unpublished).
[13]C. K. Baker and J. R. Reynolds, J. Electroanal. Chem. **251**, 307 (1988).
[14]J. B. Schlenoff and J. C. W. Chien, J. Am. Soc. **109**, 6269 (1987).
[15]E. W. Tsai, T. Pajkossy, K. Rajeshwar, and J. R. Reynolds, J. Phys. Chem. **92**, 3560 (1988).
[16]P. Kirkegaard and M. Eldrup, Comput. Phys. Commun. **7**, 401 (1974).
[17]S. E. Doyle, G. M. B. M. Jones, and R. A. Pethrick, Polym. Commun. **26**, 262 (1985).
[18]J. P. Travers, P. Audebert, and G. Bidan, Mol. Cryst. Liq. Cryst. **118**, 149 (1985).
[19]S. R. Elliott, *Physics of Amorphous Materials* (Longman, New York, 1983).
[20]N. F. Mott and E. A. Davis, *Electronic Processes in Non-Crystalline Materials* (Clarendon, Oxford, 1979).
[21]A. J. Epstein, H. Rommelmann, R. Bigelow, H. W. Gibson, D. M. Hoffman, and D. B. Tanner, Phys. Rev. Lett. **50**, 1866 (1983).
[22]W. Brandt, in *Positron Annihilation,* edited by A. T. Stewart and L. O. Roellig (Academic, New York, 1967), pp. 155.
[23]D. C. Connors and R. N. West, Phys. Lett. **30A**, 24 (1969).
[24]B. Bergersen and M. J. Stott, Solid State Commun. **7**, 1203 (1969).
[25]M. Eldrup in *Proceedings of the Sixth International Conference on Positron Annihilation, Arlington, 1982,* edited by P. G. Coleman, S. C. Sharma, and L. M. Diana (North-Holland, Amsterdam, 1982), pp. 753.
[26]S. J. Wang and Y. C. Jean, in *Positron and Positronium Chemistry, Studies in Physical and Theoretical Chemistry,* edited by D. M. Schrader and Y. C. Jean (Elsevier, Amsterdam, 1988), p. 255.
[27]S. C. Sharma, S. Berko, and W. K. Warburton, Phys. Lett. **58A**, 405 (1976).
[28]M. J. Fluss, L. C. Smedskjaer, M. K. Chason, D. G. Legnini, and R. W. Siegel, Phys. Rev. B **17**, 3444 (1978).
[29]W. L. Tanck, T. Kurschat, and T. Hehenkamp, Phys. Rev. B **31**, 6994 (1985).
[30]S. C. Sharma, R. M. Johnson, and L. M. Diana, *Nondestructive Evaluation of Metals by Positron Annihilation Techniques, Novel NDE Methods for Materials,* edited by B. B. Rath (The Metallurgical Society, AIME, Warrendale, PA, 1983), pp. 45–61.
[31]W. Brandt H. F. Waung, and P. W. Levy, Phys. Rev. Lett. **26**, 496 (1971).
[32]Y. C. Jean, T. C. Sandreczki, and D. P. Ames, J. Poly. Sci. **24**, 1247 (1986).
[33]L. H. Van Vlack, *Elements of Materials Science* (Addison-Wesley, Reading, Mass., 1964), p. 420.
[34]L. C. Smedskjaer, D. G. Legnini, and R. W. Siegel, J. Phys. F **10**, L1 (1980).
[35]M. Manninen and R. M. Nieminen, Appl. Phys. A **26**, 93 (1981).
[36]P. J. Schultz, K. G. Lynn, R. N. West, C. L. Snead, Jr., I. K. Mackenzie, and R. W. Hendricks, Phys. Rev. B **25**, 3637 (1982).